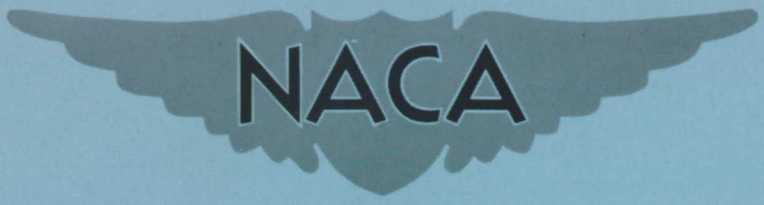

RESEARCH MEMORANDUM

FORCE AND PRESSURE-RECOVERY CHARACTERISTICS AT SUPERSONIC SPEEDS OF A CONICAL NOSE INLET WITH BYPASSES DISCHARGING OUTWARD FROM THE BODY AXIS

By Andrew Beke and J. L. Allen

Lewis Flight Propulsion Laboratory
Cleveland, Ohio

NATIONAL ADVISORY COMMITTEE
FOR AERONAUTICS
WASHINGTON

March 5, 1953
Declassified January 10, 1957

NATIONAL ADVISORY COMMITTEE FOR AERONAUTICS

RESEARCH MEMORANDUM

FORCE AND PRESSURE-RECOVERY CHARACTERISTICS AT SUPERSONIC SPEEDS OF A CONICAL NOSE INLET WITH BYPASSES DISCHARGING OUTWARD FROM THE BODY AXIS

By Andrew Beke and J. L. Allen

SUMMARY

An axially symmetric spike-type nose inlet with fixed-area bypasses located on the top and bottom of the model was investigated in the Lewis 8- by 6-foot supersonic tunnel. Each bypass was designed to discharge approximately 10 percent of the inlet capture mass flow outward from the body axis. Force and pressure-recovery data were obtained for flight Mach numbers of 1.6, 1.8, and 2.0 for a range of angles of attack from 0° to 9°.

At a Mach number of 2.0 and critical inlet flow, the configuration attained a maximum pressure recovery of 0.825 and discharged approximately 25 percent of the inlet mass flow through the bypasses. The drag for this condition was approximately twice the value obtained for a similar configuration but with bypass discharge in an axial direction. The critical drag value was about the same as that attained for equivalent inlet normal-shock spillage for a configuration without bypasses. At similar engine mass-flow ratios, the lift and pitching-moment coefficients were slightly higher than the coefficients for a configuration without bypasses.

INTRODUCTION

The off-design performance of a fixed-geometry supersonic inlet characteristically suffers large increases in drag because of mass-flow spillage behind a normal shock, or substantial losses in pressure recovery, if the inlet operation is supercritical. A simple way to alleviate these losses is to incorporate in the design a bleed which expels air in excess of engine requirements through a variable area bypass system. The diffuser may thus operate at optimum performance over a range of mass flows.

The investigation of reference 1 demonstrated that such a bypass system could substantially reduce the off-design drag increases without appreciable losses in pressure recovery. In that experiment, the bypasses were designed to discharge the excess air in nearly the axial direction. In the practical configuration, axial discharge may be difficult to incorporate and, hence, the gains to be accomplished with a bypass system may be nullified by increases in drag accompanying higher discharge angles. Calculation of these drag penalties is uncertain because of the interactions between the external stream and that of the bypass discharge. The increased pressure field due to deflection of the external stream could feasibly react on the boundary layer to separate the internal duct flow, and hence decrease the angle of bypass discharge from the calculated value. Such interaction would, of course, be favorable. In addition, in configurations with nonaxial discharge complicating interactions including mixed subsonic and supersonic flow fields in the discharge passage can occur. Only in the small angle of discharge case is the flow field amenable to calculation by the method of characteristics. The presence of a boundary layer on the walls of the bypass duct, even without interaction, renders the determination of the mean momentum direction by characteristics in a three-dimensional skewed nozzle tedious and complicated.

Nevertheless, a designer must know the relative importance of details in the design configuration which might prevent the discharge of the bypass air from being in the axial direction. An experimental configuration was therefore designed which would have a nonaxial discharge direction. The experimental results on this configuration, which were obtained at the NACA Lewis laboratory, are presented herein.

Aerodynamic and pressure-recovery characteristics of the configuration are presented for a range of mass-flow ratios at flight Mach numbers of 1.6, 1.8, and 2.0 at angles of attack up to 9°.

SYMBOLS

The following symbols are used in this report:

A area

A_m maximum external cross-sectional area

C_D drag coefficient, external drag plus internal and external drag due to bypassing mass flow, $\frac{D}{q_0 A_m}$

C_L lift coefficient, $\frac{\text{measured lift minus internal lift due to engine mass flow}}{q_0 A_m}$

C_M pitching-moment coefficient about base of model, $\frac{\text{total minus internal pitching moment due to engine mass flow}}{q_0 A_m l}$

C_{T-D} thrust-minus-drag coefficient, $\frac{T-D}{q_0 A_m}$

D drag force

L length of subsonic diffuser, 46.9 in.

l over-all length of model, 58.7 in.

M Mach number

m mass flow

m_4/m_0 engine mass-flow ratio, $\frac{\text{engine mass flow}}{\rho_0 V_0 A_1}$

m_b/m_0 bypass mass-flow ratio, $\frac{\text{bypass mass flow}}{\rho_0 V_0 A_1}$

P total pressure

p static pressure

q dynamic pressure, $\frac{\gamma p M^2}{2}$

T thrust, net force in flight direction due to change of momentum of engine mass flow between free stream (station 0) and diffuser discharge (station 4) including force on base of balance

V velocity

x longitudinal station, in.

α nominal angle of attack, deg

γ ratio of specific heats for air

ρ mass density of air

Subscripts:

x	longitudinal station
0	free stream
1	leading edge of cowl
4	diffuser discharge at constant diameter section, station 46.9
4,1	diffuser discharge at constant diameter section (sting out), station 46.9

Pertinent areas:

A_m	external maximum cross-sectional area, 0.360 sq ft
A_1	inlet capture area defined by cowl lip (measured), 0.155 sq ft
A_4	flow area at diffuser discharge, 0.289 sq ft
$A_{4,1}$	flow area at diffuser discharge (sting out), 0.338 sq ft

APPARATUS AND PROCEDURE

A schematic diagram of the model is shown in figure 1. The configuration, which is identical to the model of reference 1, except for the bypass installation, consisted of a single-conical-shock inlet without internal contraction, an annular subsonic diffuser, and two fixed-area bypasses. Tip projection of the 25° half-cone was selected so that the conical shock would intersect the leading edge of the cowl at a flight Mach number of 2.0. The slope of the cowl lip external surface was designed to be nearly alined with the local streamline behind the oblique shock. Coordinates of the cowl and centerbody are presented in table I.

The two fixed-area bypasses for discharging mass flow outward from the body axis were located approximately 6 inlet diameters downstream of the inlet entrance and on the upper and lower surfaces of the model used in reference 1. Typical cross sections of the bypass inserts, hereinafter called bypasses or nozzles, appear in figure 2. The flow passage was an asymmetric convergent-divergent nozzle formed by a filler block with an arbitrary contour fitted to the original bypass insert of reference 1. Each bypass was designed, as discussed in reference 1, to spill approximately 10 percent of the critical inlet captured mass flow.

The longitudinal area variation for the subsonic diffuser, as shown in figure 3, is the quotient of the local flow area based on the average normal to the centerbody and shell surfaces divided by the maximum flow area at the diffuser discharge station.

The model was sting-mounted from the tunnel strut. Forces were measured by an internal three-component strain-gage balance. The pressure acting on the base of the balance was measured by means of a static tube. Observed angles of attack were corrected with normal and moment readings and a static calibration of sting deflections. The actual variation of angle of attack was approximately 0.4° greater than the indicated nominal angles; however, all data were calculated for the nominal angles of attack. The regions of inlet instability, or pulsing, were determined from oscillograph recordings of axial force variations and from schlieren photographs.

The mass flow available to the engine and the amount discharged through the bypass nozzles are expressed as ratios based upon the maximum inlet capture mass flow. The engine mass flow differs from the inlet mass flow by the amount discharged through the bypasses. Engine mass-flow ratios were computed from the average static pressures at the plane of survey (station 36.7, fig. 1), while the bypassed mass-flow ratios were obtained using the average static pressures in the convergent section of the bypass nozzle. A complete discussion of the methods of instrumentation and data reduction for the inlet performance appears in references 1 and 2. The uncertainty in the value of engine mass flow resulting from the instrumentation and assumptions is 2 percent at zero angle of attack and 3 percent at 9°.

The Mach numbers at station 46.9 ($M_{4,1}$), calculated with the support sting removed, were obtained by using isentropic one-dimensional flow relations in adjusting the Mach numbers at the plane of survey (station 36.7) for the area enlargement resulting from additional divergence (stations 36.7 to 46.9) and the removal of the sting support.

The thrust-minus-drag coefficients were calculated from the strain-gage balance readings and correspond to the sum of the internal and external forces on the model in the flight direction with the sting removed. The measured thrust-minus-drag values were obtained by resolving the components of the axial and normal strain-gage balance readings at each angle of attack. Since the over-all thrust of the propulsive unit is composed of the net forces of the inlet diffuser, engine, and exit nozzle, this coefficient may be used directly in computing inlet-engine performance. The drag was established by subtracting the measured thrust-minus-drag from the computed thrust resulting from the change of momentum in the flight direction of the engine mass flow between the free stream and the diffuser exit.

The drag coefficient includes the external drag of the model and the net internal and external momentum change in the flight direction of the bypass mass flow. The lift and pitching-moment coefficients were calculated by subtracting the difference between the measured forces and the computed internal lift or pitching moment, respectively, due to the engine mass flow. The internal and external effects of bypass mass flow and the additive components due to inlet spillage are retained in these coefficients, as in the drag coefficients. Pitching-moment and lift coefficients were computed on the basis of the turning of the engine mass flow at the cowl lip.

RESULTS

A schlieren photograph of the flow field downstream of the bypass exit is presented in figure 4. This figure demonstrates that the interaction between the internal and external flow was so intensive that strong shocks with mixed subsonic and supersonic flow regions occurred in the bypass duct. The force and pressure-recovery characteristics obtained with bypass mass flow discharged outward from the body axis are presented in figures 5 to 7 for Mach numbers of 1.6, 1.8, and 2.0 and for nominal angles of attack up to 9°. The variation of bypass mass-flow ratio, diffuser total-pressure recovery, and diffuser-discharge Mach number are presented as functions of engine mass-flow ratio. Variation of thrust-minus-drag and resulting drag coefficients (which include the drag associated with bypassing) are also presented. The change of pitching-moment coefficient and lift coefficient with engine mass-flow ratios appears in figure 8 for the entire range of flight Mach number and angle of attack.

DISCUSSION

Drag. - The total drag at critical inlet flow, for the design-point condition (Mach number, 2.0; zero angle of attack; engine mass-flow ratio, 0.750) was 0.200 (fig. 5). This value is 0.085 greater than the drag at the same conditions for the axial discharge model and is about 0.105 greater than the critical drag for a similar configuration which has no bypasses. The higher drag for the outward bypass discharge, as compared with the axial-discharge case, results from loss of part of the bypass exit momentum due to the larger effective bypass discharge angle. Secondary effects, which result from slight changes of the pressure and friction-drag characteristics of the nacelle, may also contribute to the larger drag value.

An estimate was made to determine the effect of complete loss (normal discharge) of the free-stream bypass momentum on the drag. The calculated value of the incremental drag coefficient (additional drag greater than critical drag for a configuration without bypasses) for a bypass

mass-flow ratio of 0.250 was 0.216, which would result in a maximum critical drag value of 0.311 if normal bypass discharge were attained. In view of this estimate and the data of figure 5(b), it is therefore apparent that, if a bypass system is to be employed for engine mass-flow control, discharge of the excess mass flow in an axial direction is desirable, and that designs which do not approximate axial discharge will probably have poor performance.

In figure 5(b) the critical drag value (engine mass-flow ratio of 0.750) is approximately equal to the drag for an inlet without bypasses operating at the same engine mass-flow ratio. However, the coincidence of the drag due to outward discharge and the additive drag for inlet normal-shock spillage is a singular result and is a characteristic of the effective discharge angle of this configuration. For larger effective bypass discharge angles, the drag curve would probably translate upward so that the entire range of drag values would be greater than for inlet normal-shock spillage. At engine mass flows greater than 0.750 (fig. 5(b)), the drag values decrease as a result of decreasing bypass mass-flow ratios.

In general, the drag coefficients in the region of critical inlet flow do not change appreciably with Mach number. However, at a given Mach number, the drag values increase with increased angle of attack because of induced drag.

Thrust-minus-drag. - The thrust-minus-drag coefficient for the design-point condition (Mach number, 2.0; zero angle of attack; engine mass-flow ratio, 0.750) was 0.925 (fig. 5(b)) and represents a reduction of approximately 14 percent of the thrust-minus-drag compared with the axial discharge case (ref. 1). At zero angle of attack and Mach numbers of 1.8 and 1.6, the thrust-minus-drag coefficients, compared with axial discharge, decreased uniformly in approximately the same ratio as at a Mach number of 2.0. Since the pressure-recovery and mass-flow characteristics of the inlet are nearly the same as for reference 1 (see Inlet performance), these reductions result from the turning of the bypassed air outwards, the external effects accompanying outward discharge, and the small difference in the internal momentum losses of the bypassed air for the two cases.

Lift and pitching moment. - The variations of lift and pitching-moment characteristics in figure 8 are similar to those of reference 2. Inasmuch as the axial discharge case (ref. 1) had bypasses located on the sides of the model, and since there is a difference in the flow disturbance downstream of the bypasses for reference 1 and this investigation, no valid comparison at angles of attack can be made between the two cases to determine the effects of discharge angle. At all Mach numbers and angles of attack, the magnitudes of the critical flow values for the bypass discharge are slightly higher than the values for the case without bypasses (ref. 2). The same result is noted when comparison is

made at angles of attack of 3° and 6° for engine mass-flow ratios less than 0.775. The increased lift can be attributed primarily to the internal lift associated with the bypass mass flow, whereas negligible lift contribution is attributed to the additive components for inlet normal-shock spillage.

Inlet performance. - At the design Mach number, zero angle of attack, and subcritical flow, approximately 25 percent of the maximum inlet captured mass flow was discharged through the fixed-area bypasses. In the region of stable subcritical inlet flow, the bypass mass-flow ratio remained fairly insensitive to angle of attack and decreased with Mach number (figs. 5(a) and 7(a)). At each Mach number and angle of attack, the bypass discharged nearly a constant mass flow in the subcritical region. Discussion of the internal flow properties regulating the bypass operation appears in reference 1. A maximum diffuser total-pressure recovery of 0.825 was attained at critical inlet flow for a Mach number of 2.0 and zero angle of attack (fig. 5(a)). For the same condition (Mach number, 2.0; zero angle of attack), a stable subcritical operating range between engine mass flows of 0.750 and 0.375 was obtained. No pulsing was observed at the off-design Mach numbers. In general, the pressure-recovery and mass-flow characteristics of the inlet are in agreement with the results of reference 1 for the entire range of Mach numbers and angles of attack.

SUMMARY OF RESULTS

An investigation of the force and pressure-recovery characteristics of a nacelle-type conical spike-inlet model with two fixed-area bypasses designed to discharge mass flow outward from the model axis indicated the following results:

1. For critical inlet flow at a Mach number of 2.0 and zero angle of attack, the drag was nearly twice the value obtained for a similar model which discharged about the same mass flow in an axial direction. The critical drag value was approximately equal to the drag for an inlet without bypasses operating at the same engine mass flow with normal-shock spillage. Thus attention must be paid to design details of a bypass system to assure axial or nearly axial discharge of the bypassed air.

2. At all Mach numbers and angles of attack and similar engine mass flows, the lift coefficients were slightly increased as a result of bypassing.

3. The bypass discharged nearly a constant mass flow for subcritical inlet flow at each Mach number and angle of attack investigated. The

bypass mass flow and diffuser pressure recovery were about the same as the values obtained for a similar model with bypasses discharging in an axial direction.

Lewis Flight Propulsion Laboratory
National Advisory Committee for Aeronautics
Cleveland, Ohio

REFERENCES

1. Allen, J. L., and Beke, Andrew: Force and Pressure Recovery Characteristics at Supersonic Speeds of a Conical Spike Inlet with Bypasses Discharging in an Axial Direction. NACA RM E52K14, 1953.

2. Beke, Andrew, and Allen, J. L.: Force and Pressure-Recovery Characteristics of a Conical-Type Nose Inlet Operating at Mach numbers of 1.6 to 2.0 and Angles of Attack up to 9°. NACA RM E52I30, 1952.

TABLE I - COORDINATES

Centerbody		Cowling		
Station (in.)	Radius (in.)	Station (in.)	External radius (in.)	Internal radius (in.)
-2.86	[a]0	0	2.671	2.671
- .2	[a]1.24	.015	2.686	2.656
.0	1.32	.5	2.79	2.73
.1	1.36	1.0	2.89	2.80
.2	1.39	1.5	2.97	2.86
.3	1.42	2.0	3.04	2.92
.4	1.45	2.5	3.11	2.98
.5	1.48	3.0	3.16	3.03
.8	1.56	4.0	3.25	3.12
1.0	1.61	5.0	3.32	3.20
1.5	1.73	6.0	3.38	3.25
2.0	1.84	7.0	3.42	3.30
2.5	1.92	8.0	3.45	3.33
3.0	2.01	8.67	3.47	3.35
4.0	2.14			
5.0	2.24			
6.0	2.31			
7.0	2.37			
8.0	2.42			
9.0	2.44			
10.0	2.46			
12.0	2.46			
14.0	2.44			
16.0	2.40			
18.0	2.32			
20.0	2.19			
22.4	2.03			
24.0	1.95			
28.0	1.75			
32.0	1.61			
37.1	1.50			
46.9	1.50			

[a]Region of 25°-half-angle cone.

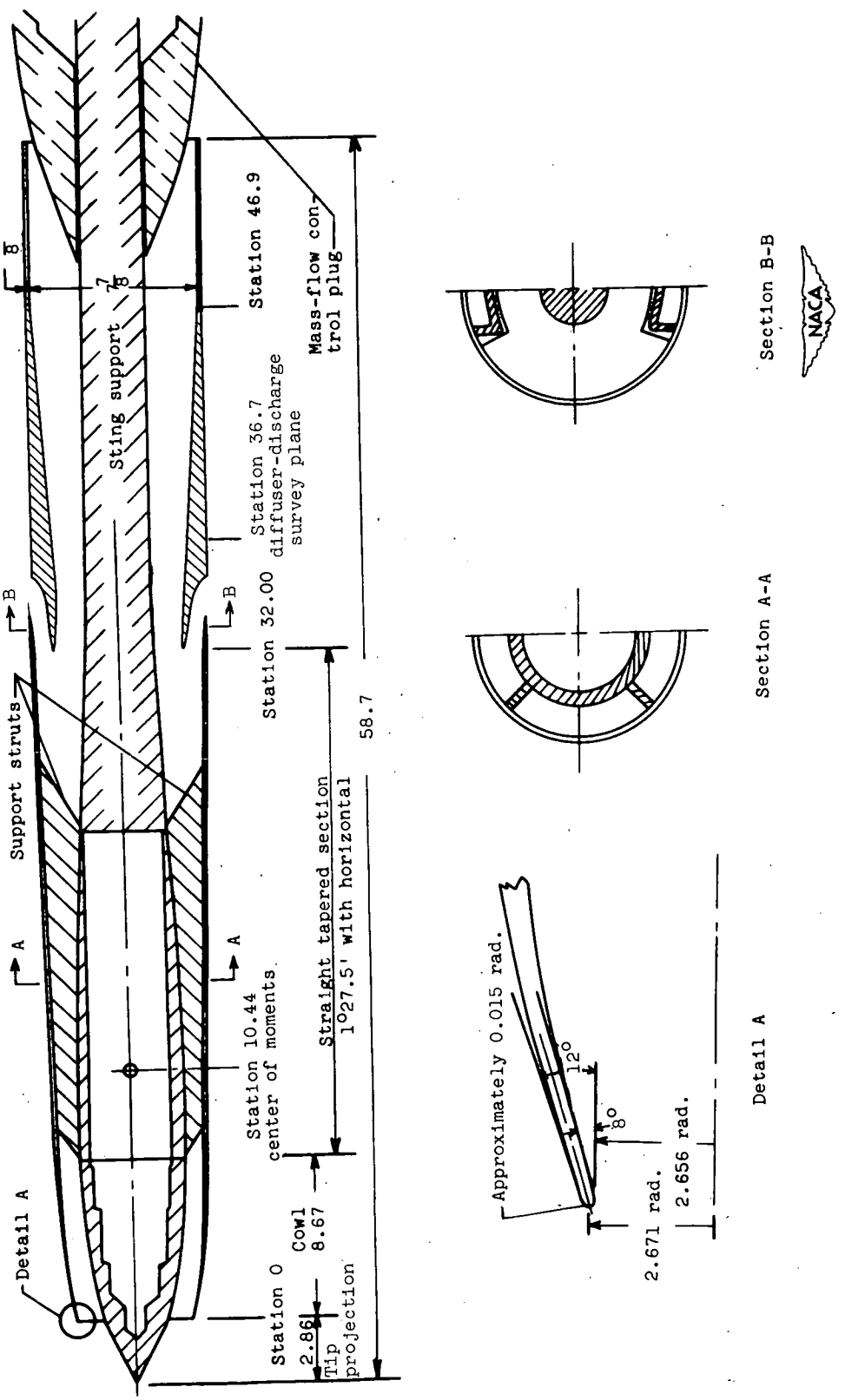

Figure 1. - Schematic diagram of elevation form of model. (All dimensions in inches.)

x	y	z	Flow area
0	3.63	0.94	3.50
.2	3.30	.788	2.62
.4	3.18	.712	2.40
.6	3.08	.660	2.22
.8	3.02	.627	2.03
.9	3.02	.618	1.90
1.0	3.02	.604	1.82
1.25	3.02	.650	1.97
1.64	3.02	.700	2.07

θ	R
0	1.125
9	1.040
27	.940
41	.845
55	.740
79	.712

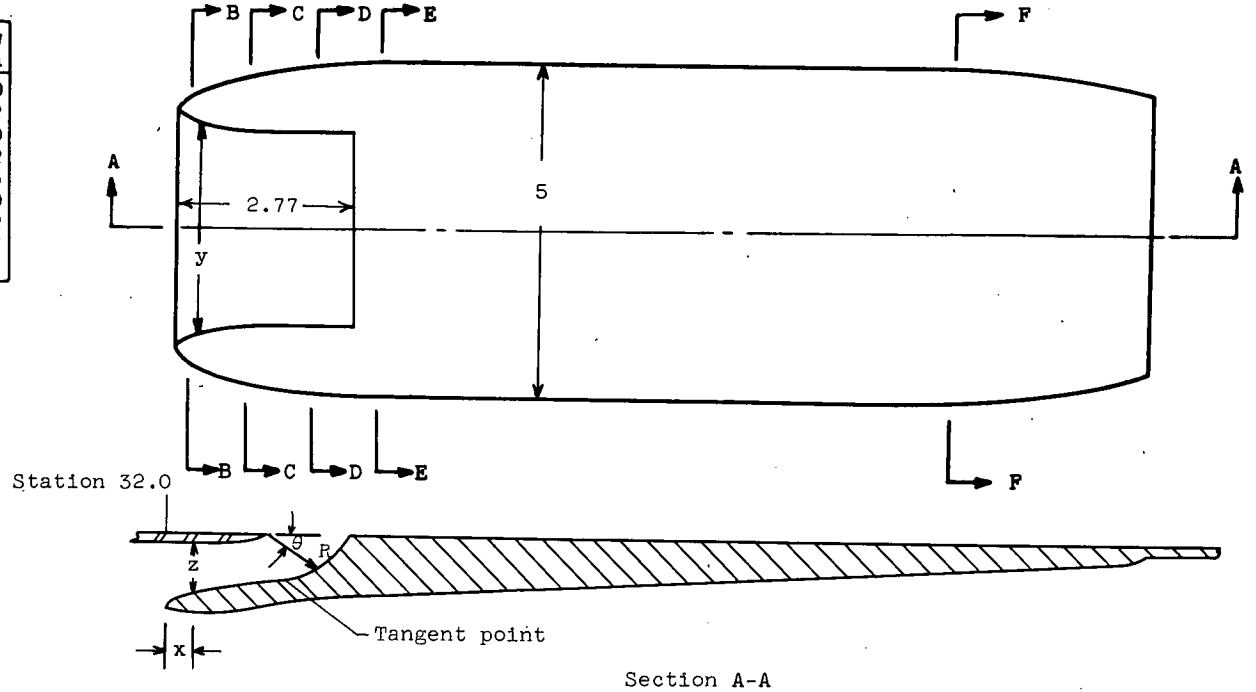

Section A-A

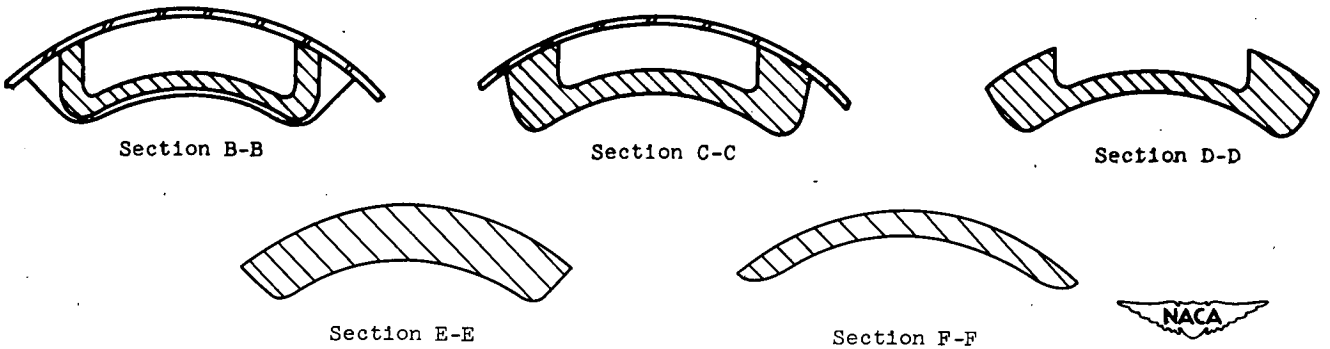

Figure 2. - Details of outward discharge bypass. (All dimensions in inches.)

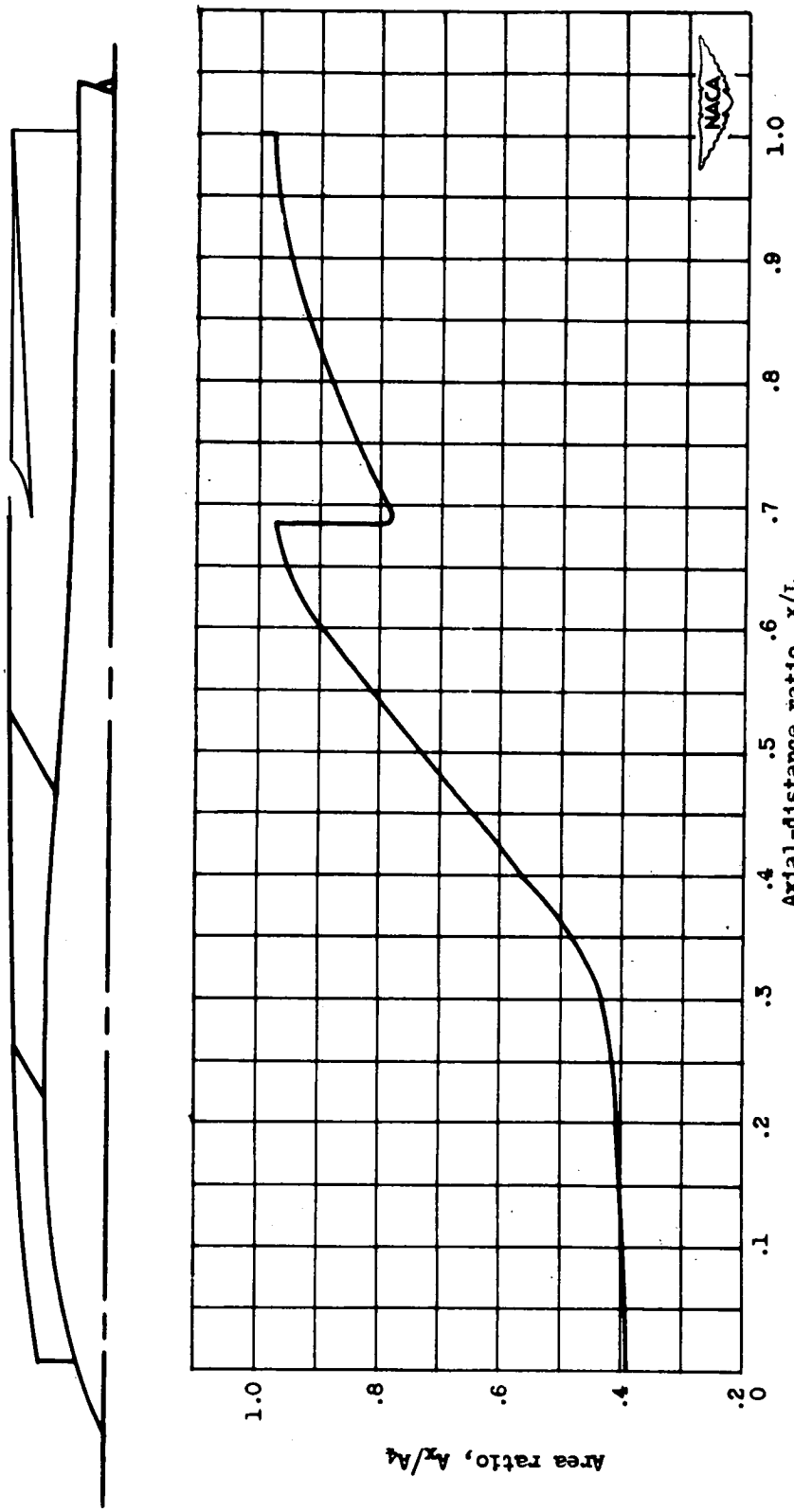

Figure 3. - Subsonic-diffuser area variation.

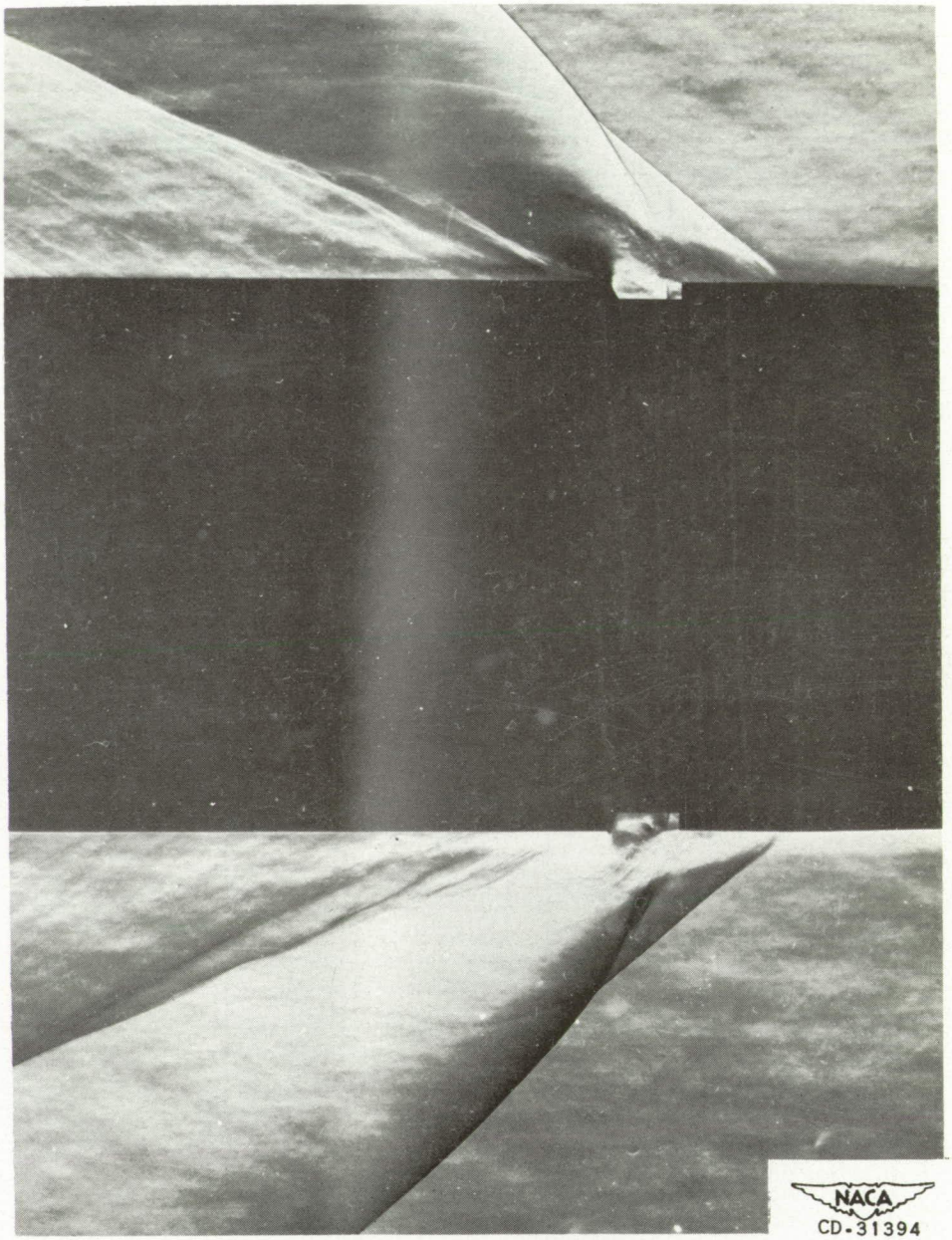

Figure 4. - Schlieren photograph of bypass-exit flow field for bypass mass-flow ratio of 0.25 and critical inlet flow. Mach number, 2.0; zero angle of attack.

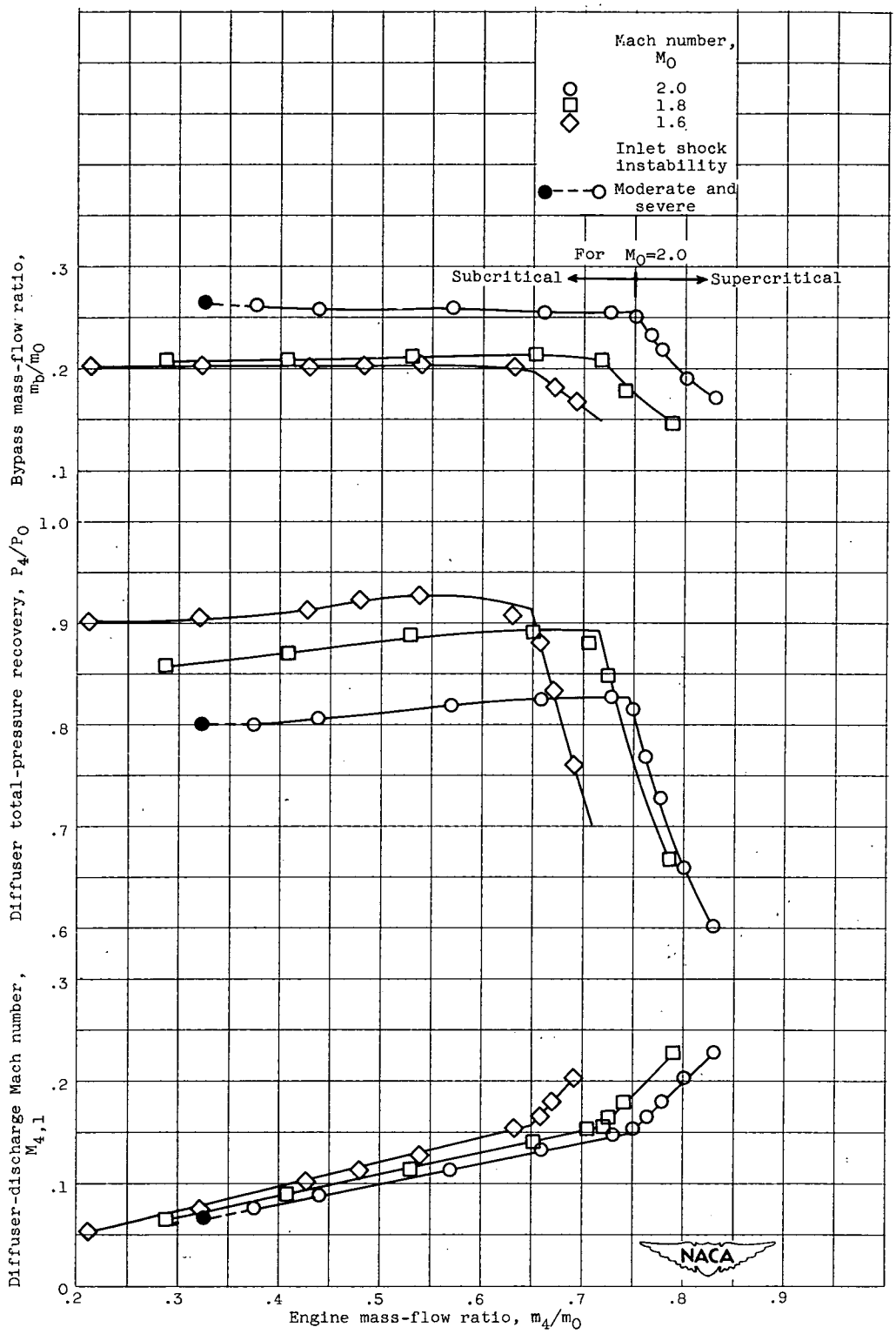

(a) Inlet characteristics.

Figure 5. - Variation of inlet characteristics and force coefficients with engine mass-flow ratio for range of Mach number at zero angle of attack.

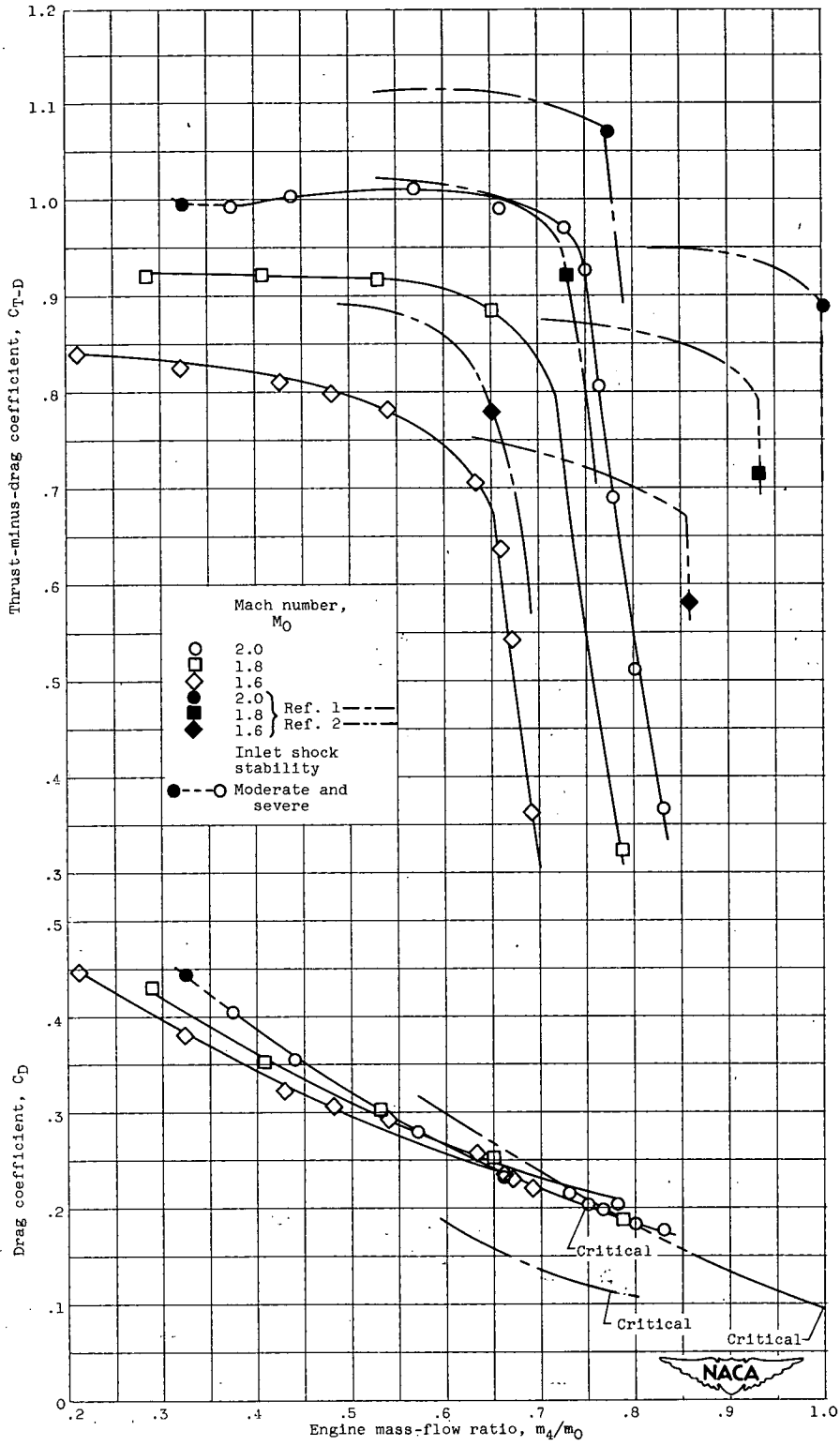

(b) Force coefficients.

Figure 5. - Concluded. Variation of inlet characteristics and force coefficients with engine mass-flow ratio for range of Mach number at zero angle of attack.

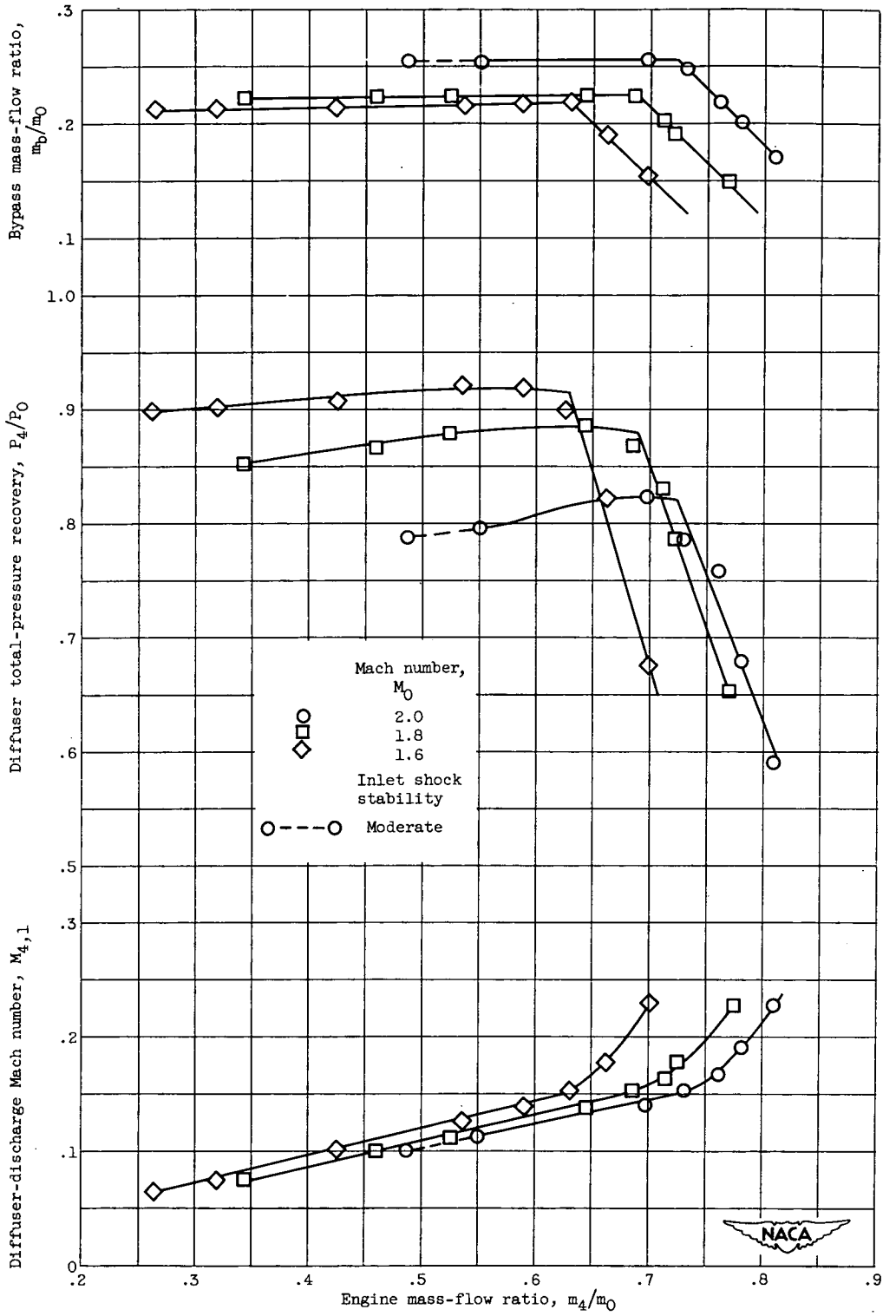

(a) Inlet characteristics.

Figure 6. - Variation of inlet characteristics and force coefficients with engine mass-flow ratio for range of Mach number at nominal angle of attack of 6°.

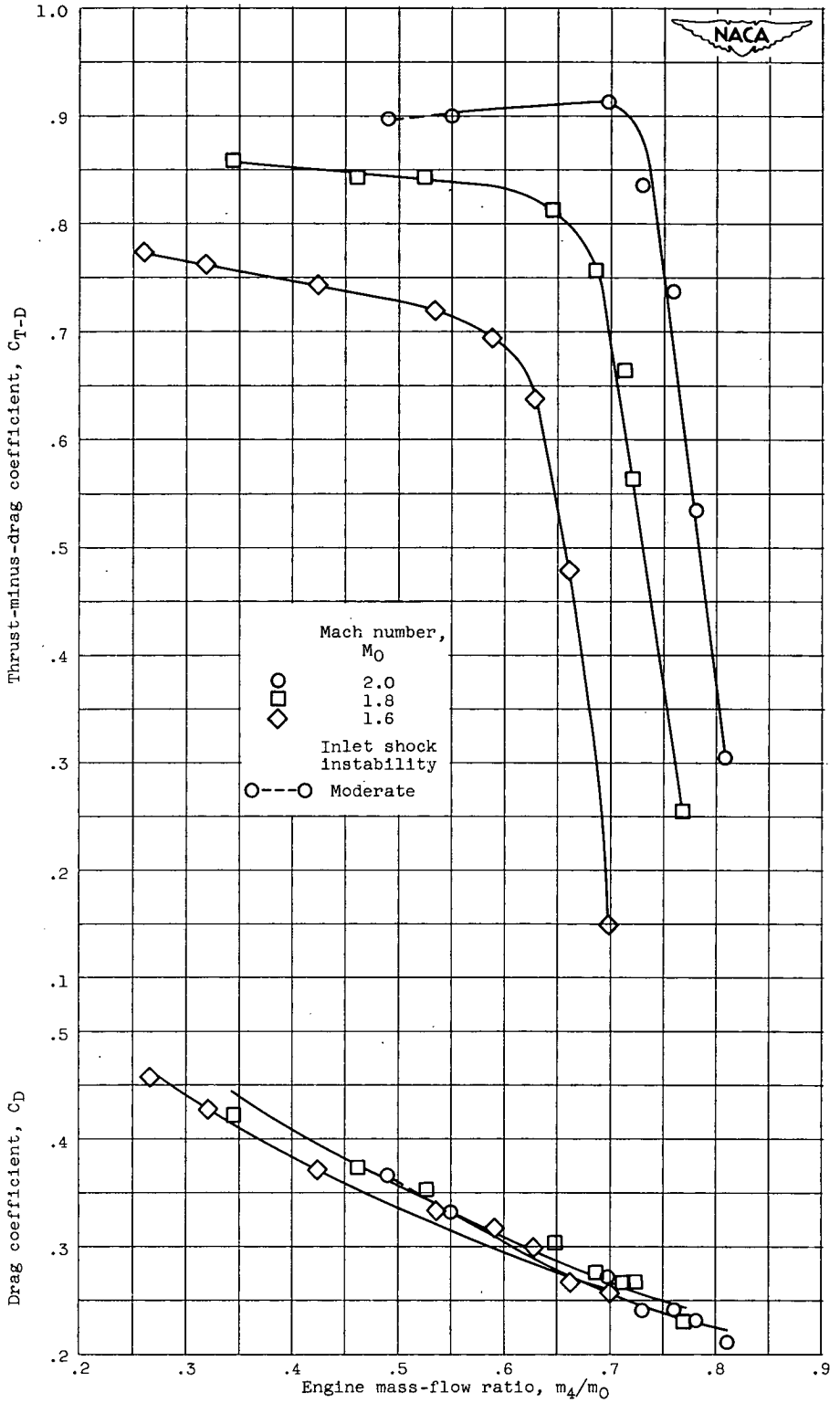

(b) Force coefficients.

Figure 6. - Concluded. Variation of inlet characteristics and force coefficients with engine mass-flow ratio for range of Mach number at nominal angle of attack of 6°.

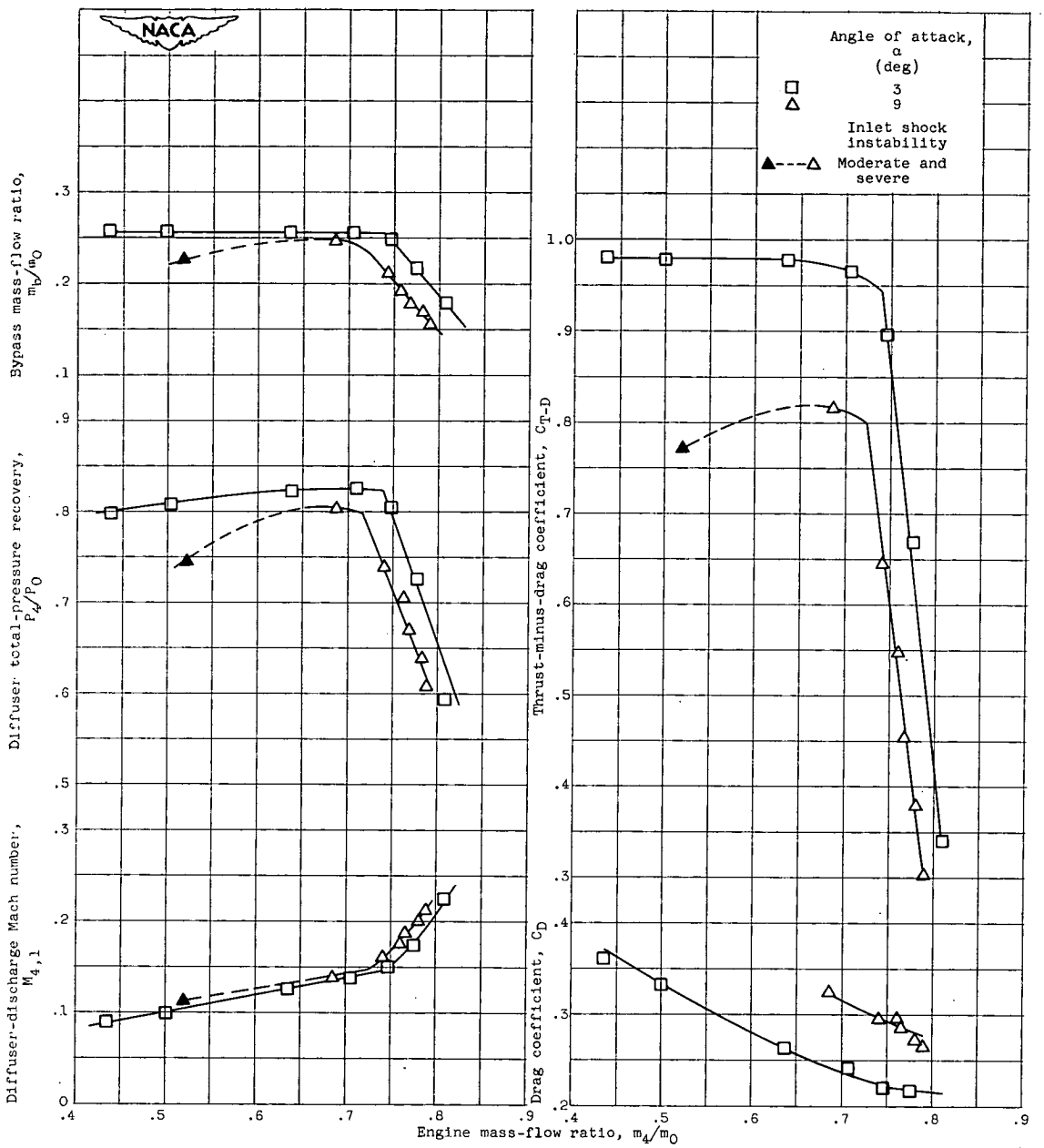

(a) Inlet characteristics. (b) Force coefficients.

Figure 7. - Variation of inlet characteristics and force coefficients with mass-flow ratio for Mach number of 2.0 at nominal angles of attack of 3° and 9°.

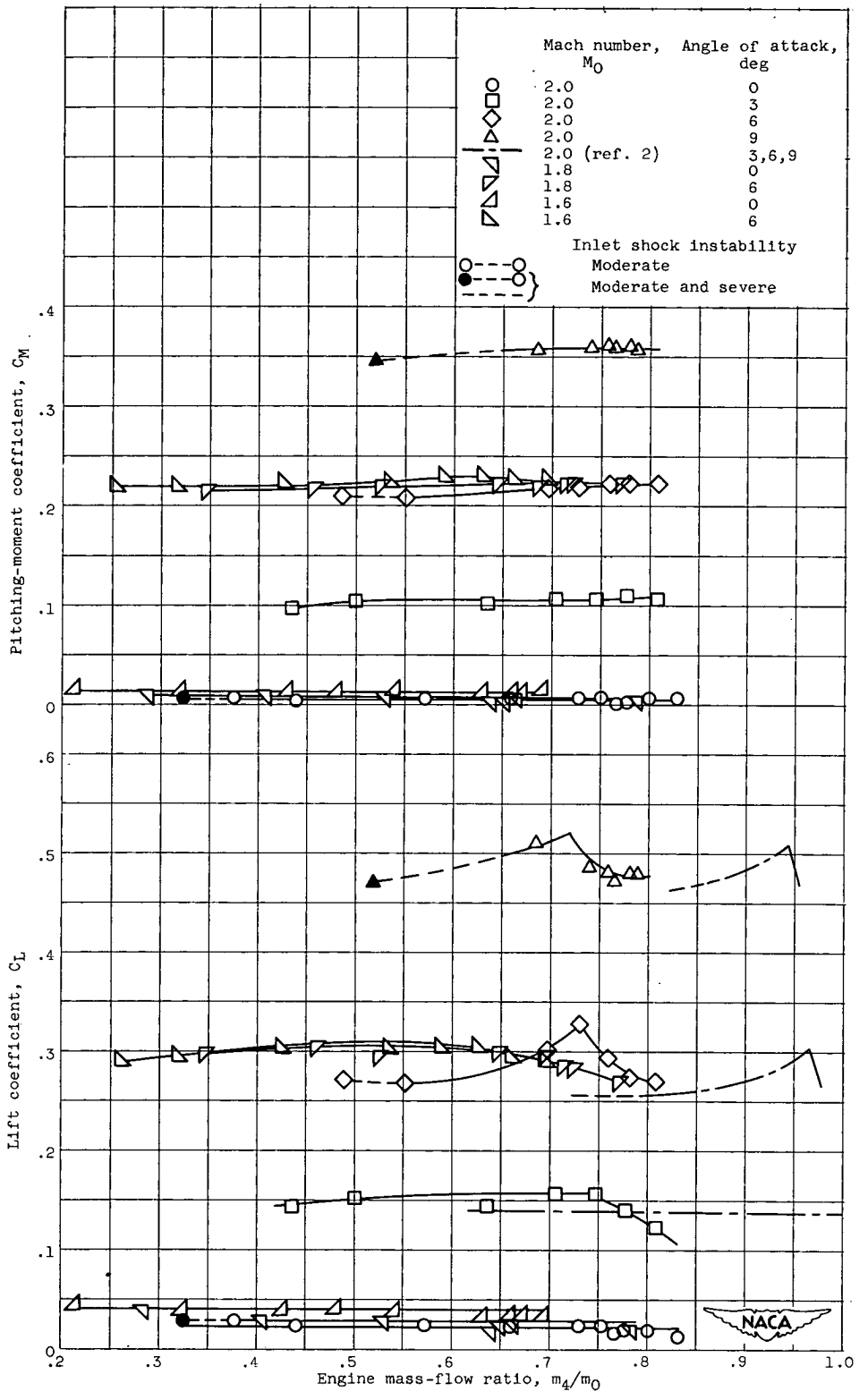

Figure 8. - Variation of lift and pitching-moment coefficients with engine mass-flow ratio for range of Mach number at nominal angles of attack of 0°, 3°, 6°, and 9°.